

Wintertime nitrate formation pathways in the North China Plain:
Importance of N₂O₅ heterogeneous hydrolysis

Lang Liu^{1,4}, Naifang Bei², Bo Hu³, Jiarui Wu^{1,4}, Suixin Liu^{1,4}, Xia Li^{1,4}, Ruonan Wang^{1,4}, Zirui Liu³,
Jiaoyang Yu¹, Min Zuo^{1,4}, Zhenxing Shen², Junji Cao^{1,4}, Xuexi Tie¹, and Guohui Li^{1,4*}

¹Key Lab of Aerosol Chemistry and Physics, SKLLQG, Institute of Earth Environment, Chinese Academy of Sciences, Xi'an, 710061, China

²School of Human Settlements and Civil Engineering, Xi'an Jiaotong University, Xi'an, 710049, China

³State Key Laboratory of Atmospheric Boundary Layer Physics and Atmospheric Chemistry, Institute of Atmospheric Physics, Chinese Academy of Sciences, Beijing, 100029, China

⁴CAS Center for Excellence in Quaternary Science and Global Change, Xi'an, 710061, China

* Correspondence to: Guohui Li (liqh@ieecas.cn)

Abstract: Nitrate aerosols, formed via nitric acid (HNO₃) to balance inorganic cations in the particle phase, have constituted a major fraction of fine particulate matters (PM_{2.5}) during wintertime haze events in the North China Plain (NCP), with a progressively increasing contribution to PM_{2.5} mass. HNO₃ is produced through homogeneous and heterogeneous pathways in the atmosphere, but the contribution of the two pathways to nitrate remains elusive. Simulations of a wintertime haze event in the NCP using a source-oriented WRF-Chem model reveal that the homogeneous and heterogeneous pathways contribute 48.4% and 51.6% of near-surface nitrate mass on average, respectively. The heterogeneous pathway dominates the nighttime HNO₃ production in the planetary boundary layer, with an average contribution of 83%. Although N₂O₅ is photolytically liable during daytime, the heterogeneous N₂O₅ hydrolysis still contributes 10% of HNO₃. Our study highlights the significantly important role of N₂O₅ heterogeneous hydrolysis in the nitrate formation during wintertime haze days.

Plain Language Summary: Nitrate aerosols have become a major fraction of fine particulate matters during wintertime haze events in the North China Plain (NCP) with implementation of strict emission mitigation measures since 2013. We quantify the contribution of nitrate formation pathways during a wintertime haze event in the NCP using a source-oriented WRF-Chem model. The homogeneous and heterogeneous pathways dominate the nitrate formation during daytime and nighttime respectively. The N₂O₅ heterogeneous hydrolysis also plays an appreciable role in the nitrate formation even during daytime under weak sunlight and high humidity conditions.

1 Introduction

In recent ten years, persistent and pervasive haze with high levels of fine particulate matters ($\text{PM}_{2.5}$) frequently engulfs the North China Plain (NCP) during wintertime, caused by a synergy of massive anthropogenic emissions and atmospheric processes (An et al., 2019). High loadings of $\text{PM}_{2.5}$ in the atmosphere not only adversely affect human health, ecosystems, and visibility, also perturb regional weather and climate (Lelieveld et al., 2015; IPCC, 2013). Therefore, since 2010, the Chinese government has made great efforts to decrease emissions of air pollutants, and the air quality has been improved considerably (Zheng et al., 2018; Zhang et al., 2019). However, field observations have demonstrated that the nitrate contribution to $\text{PM}_{2.5}$ mass has progressively increased and nitrate aerosols have constituted a major fraction of $\text{PM}_{2.5}$ in recent several years (Tao et al., 2017; Sun et al., 2015; Zhang et al., 2013).

Nitrate aerosols are formed via nitric acid (HNO_3) to balance inorganic cations in the particle phase, which is mainly produced through the homogenous pathway of $\text{OH} + \text{NO}_2$ and the heterogeneous pathway of the N_2O_5 heterogeneous hydrolysis uptake on surfaces of deliquescence aerosols (Chang et al., 2016; Brown et al., 2016; Lowe et al., 2015; Chang et al., 2011; Bertram & Thornton, 2009). The N_2O_5 hydrolysis is the most important pathway during nighttime since N_2O_5 is photolytically liable, or even plays a considerable role in nitrate formation during heavy haze events with weak sunlight and high relative humidity (RH) (Brown et al., 2016).

Xue et al. (2014) have reported the average nitrate production rate of $1.36 \mu\text{g m}^{-3} \text{h}^{-1}$ based on field observations during haze events in Hong Kong. According to N_2O_5 measurements in Beijing, Wang et al. (2017) have estimated that the potential nitrate contribution of the N_2O_5 hydrolysis is about 52%. Using the stable isotope analysis method, Wang et al. (2019) have found that the homogeneous and heterogeneous pathways contribute

66% and 34% of the nitrate mass in Beijing, respectively. Model simulations have further highlighted the importance of the N_2O_5 hydrolysis to nitrate formation (Riemer et al., 2003; Kim et al., 2014; Lowe et al., 2015; Liu et al., 2019). However, those model evaluations are generally based on the brute force method (BFM), i.e. turning off the homogeneous or heterogeneous pathway in simulations. The BFM can be used to evaluate the importance of the certain pathway, but has flaws in quantifying its contribution, considering interactions of complicated physical and chemical processes in the atmosphere (Zhang & Ying, 2011).

The source-oriented method coupled with air quality models (AQMs) can track the formation of particulate and gas pollutants produced from various sources or pathways through one mathematical simulation of emissions, chemical reactions, gas-to-particle conversion, transport and deposition (Ying & Kleeman, 2006). The source-oriented AQMs have been widely used to quantify contributions of emission sources or formation pathways to $\text{PM}_{2.5}$ or ozone (O_3) (Ying & Krishnan, 2010; Zhang & Ying, 2011; Hu et al., 2012; Hu et al., 2015; Hu et al., 2017; Wang et al., 2018; Ying et al., 2018; Qiao et al., 2018; Liu et al., 2019). However, the quantitative study of nitrate formation pathways based on the source-oriented AQMs has rarely been reported.

In the present study, a source-oriented WRF-Chem model has been developed and applied to quantify contributions of homogeneous and heterogeneous pathways to nitrate formation during wintertime of 2016 in the NCP.

2 Model and method

2.1 WRF-Chem model and configuration

The source-oriented AQM used in the study is based on a specific version of the WRF-Chem model (Grell et al., 2005) with modification by Li et al. (2010; 2011a; 2011b; 2012). The specific WRF-Chem model includes a flexible gas phase chemical module with

consideration of different chemical mechanisms and the CMAQ aerosol module (AERO5) developed by US EPA (Foley et al., 2010). The organic aerosols (OA) are simulated using the volatility basis-set (VBS) modeling method, with the secondary OA (SOA) contributions from glyoxal and methylglyoxal. ISORROPIA (Version 1.7) is used to predict the inorganic aerosols, calculating the composition and phase state of an ammonium-sulfate-nitrate-water inorganic aerosol in thermodynamic equilibrium with gas phase precursors (Nenes et al., 1998). Detailed description about the specific WRF-Chem model can be found in Supporting Information (SI).

The source-oriented method introduces additional chemical species to represent formations from various pathways, providing a direct and quantitative determination of the contribution of each pathway (Ying & Krishnan, 2010). A detailed description of the method can be found in previous studies (Ying & Kleeman, 2006; Ying & Krishnan, 2010; Zhang & Ying, 2011). In the atmosphere, the reactions of OH with NO₂, NO₃ with hydrocarbons (HCs), and the N₂O₅ heterogeneous hydrolysis dominate the HNO₃ formation. In the study, two reactive tagged gas-phase species (HNO₃_A and HNO₃_B) are introduced to track the homogeneous and heterogeneous HNO₃ formation, respectively (Table S2), and the corresponding aerosol-phase species (ANO₃_A and ANO₃_B) are also introduced to trace the nitrate aerosol formation from each pathway. The detailed reactions of HNO₃_A and HNO₃_B can be found in Table S1. We use ISORROPIA to distribute the NH₃/ammonium, HNO₃/nitrate, and water between the gas and aerosol phases as a function of total sulfate, total ammonia, total nitrate, relative humidity and temperature (Nenes et al., 1998). The apportionment for nitrate aerosols follows the mass conversion of **N(+VI)** from each formation pathway, when the total nitrate is distributed between the gas and aerosol phases by ISORROPIA after one time step integration, as shown in Figure 1. The reaction rate constant of N₂O₅ heterogeneous hydrolysis on surfaces of deliquescent aerosols is calculated using the

reaction probability ($\gamma_{N_2O_5}$). The parameterization of $\gamma_{N_2O_5}$ used in this study follows Riemer et al. (2009), considering effects of organic coating on the N_2O_5 hydrolysis uptake (Liu et al., 2019).

The source-oriented WRF-Chem model is used to simulate a heavy haze episode from 16 to 31 December 2016 in the NCP. Figure S1 shows the model simulation domain, and the detailed model configuration can be found in Table S2. The observation data sets used to evaluate the model performance include 3-hourly measurements of meteorological parameters in Beijing, and hourly on-line measurements of air pollutants released by Ministry of Ecology and Environment of China, and 12-hourly filter measurements of sulfate, nitrate, and ammonium in Beijing, Tianjin, Shijiazhuang and Cangzhou (Figure S1).

3 Results and Discussions

Generally, the source-oriented WRF-Chem model performs reasonably well in simulating meteorological fields, air pollutants, and inorganic aerosols compared to measurements in the NCP (Figures S2-S5). Detailed model validation can be found in SI. The good model performance provides a reliable base for further quantifying the nitrate formation pathways.

3.1 Contribution of the homogeneous and heterogeneous pathways to nitrate

Figure 2 presents the simulated temporal variation of average near-surface nitrate concentrations from the homogeneous and heterogeneous pathways in the NCP from 16 to 31 December 2016. The homogeneous and heterogeneous pathways contribute 48.4% ($15.1 \mu\text{g m}^{-3}$) and 51.6% ($16.3 \mu\text{g m}^{-3}$) of the nitrate mass on average in the NCP during the episode, respectively. During the stage of the haze formation and development from 16 to 19 December, the homogeneous pathway is the dominant nitrate source, with an average contribution of 63.0%. Meanwhile, the nitrate contribution of the heterogeneous pathway

progressively increases from around 10% to 50%. After 20 December, the heterogeneous pathway plays a more important role in nitrate formation than the homogeneous pathway, accounting for 57.0% of nitrate mass on average. Figure 3 presents the spatial distributions of average near-surface nitrate contributions of the homogeneous and heterogeneous pathways during the episode. Contributions of the homogeneous pathway to the nitrate formation are more than $12 \mu\text{g m}^{-3}$ in the NCP, exceeding $27 \mu\text{g m}^{-3}$ in the south of Hebei. Similar to the spatial distribution of the homogeneous pathway, the nitrate contribution of the heterogeneous pathway exceeds $15 \mu\text{g m}^{-3}$ in the NCP and exceeds $27 \mu\text{g m}^{-3}$ in highly industrialized cities, such as Shijiazhuang, Xingtai, and Zhengzhou.

Model results have shown that the heterogeneous pathway plays a significantly important role in nitrate formation during the haze episode, which is consistent with field observations in the NCP. Wang et al. (2017) have calculated the daily average nitrate formation potential from the heterogeneous N_2O_5 hydrolysis based on the field measurements in Beijing, reporting that the heterogeneous pathway accounts for 52% of the total nitrate formation. Moreover, Wang et al. (2019) have evaluated the different pathways to nitrate contribution in Beijing using stable oxygen isotopes analysis methods. They have found that around 34% on average and up to 54% of nitrate mass are produced by the N_2O_5 hydrolysis in winter. However, Liu et al. (2019) have evaluated nitrate contributions of the N_2O_5 hydrolysis in Beijing-Tianjin-Hebei (BTH) using the BFM based on the WRF-Chem model, showing that the N_2O_5 hydrolysis produces about 30% of nitrate mass, which is much lower than that in the present study.

In order to settle the large inconsistency, we have further used the BFM to assess nitrate contributions of the heterogeneous pathway in the present study, by differentiating simulations with and without the heterogeneous pathway (referred to as BASE and HET0 case, respectively) (Figure S6). The result demonstrates that about 30.8% of near-surface

nitrate aerosols are contributed by the heterogeneous pathway in the NCP during the episode, indicating that the BFM might not be suitable for evaluation of the importance of different pathways to nitrate formation. When both the homogeneous and heterogeneous pathways are considered in the BASE case, the HNO_3 formed from each pathway competes for inorganic cations in the particle phase, and the nitrate apportionment between the two pathways depends on the total nitrate ($N(+VI)$) produced by each pathway. However, when the heterogeneous pathway is not considered in the HET0 case, only the HNO_3 formed from the homogeneous pathway balances inorganic cations in the particle phase, without competition with that from the heterogeneous pathway. Therefore, more HNO_3 from the homogeneous pathway exists in the particle phase in the HET0 case than the BASE case. When comparing the BASE and HET0 case, the nitrate contribution of the heterogeneous pathway is underestimated, and the underestimation relies on the inorganic cations in the particle phase.

3.2 HNO_3 production rate of the homogeneous and heterogeneous pathways

Generally, the heterogeneous N_2O_5 hydrolysis mainly occurs during nighttime considering that N_2O_5 is formed from the reaction of $\text{NO}_2 + \text{NO}_3$ and NO_3 and N_2O_5 are both photolytically liable, causing very low levels of daytime N_2O_5 . The N_2O_5 heterogeneous hydrolysis constitutes the most important nitrate source during nighttime, but its role during daytime remains elusive, particularly during haze days with weak solar radiation and high RH. Furthermore, the reaction of $\text{OH} + \text{NO}_2$ dominates daytime HNO_3 production but becomes an insignificant HNO_3 source during nighttime due to the absence of OH. The NO_3 reaction with HCs has large potentials to be an important HNO_3 source because of increased NO_3 and HCs concentrations during nighttime. However, as a bulk method, ISORROPIA distributes the gas-phase HNO_3 and particulate-phase nitrate according to the total nitrate, which includes contributions of accumulation and local production. Therefore, it is not possible to determine the nitrate contribution of each pathway during daytime or nighttime using

concentrations of the tagged HNO_3 and nitrate aerosols (Figure 2).

We have further included two additional tagged species to represent the *in-situ* HNO_3 production of the homogeneous and heterogeneous pathways in the source-oriented WRF-Chem model, to provide temporal variations of the HNO_3 contribution of each pathway. Figure 4 presents the diurnal profile of the average HNO_3 production rate (P_{HNO_3}) of the homogeneous and heterogeneous pathways in the planetary boundary layer (PBL) over the NCP during the episode. The average P_{HNO_3} of the homogeneous pathway is 85.6 ppt h^{-1} in the PBL during the episode, with a HNO_3 contribution of 49.8%. On December 21 and 26, the P_{HNO_3} of the homogeneous pathway decreases significantly due to reduction in the downward solar radiation (Figure S7). Although N_2O_5 is highly photolabile, the daytime HNO_3 production rate of the N_2O_5 hydrolysis is nonzero and exceeds 25 ppt h^{-1} on December 21. The average P_{HNO_3} of the heterogeneous pathway is 86.4 ppt h^{-1} in the PBL, with a HNO_3 contribution of 50.2% in the NCP during the episode, which is a little bit higher than that of the homogeneous pathway. It is worth noting that the calculated P_{HNO_3} ratio of the homogeneous to heterogeneous pathways in the PBL are well consistent with that of the near-surface nitrate contribution between the two corresponding pathways.

Figure 5 shows the diurnal cycle of the average P_{HNO_3} of homogeneous and heterogeneous pathways in the PBL over the NCP during the episode. During nighttime, from 18:00 to 07:00 Beijing Time (BJT) of the next day, the heterogeneous pathway dominates the HNO_3 production, with an average HNO_3 contribution of 83.0%. Because of lack of OH due to absence of O_3 and peroxide photolysis, the nighttime HNO_3 contribution of the homogeneous pathway is mainly attributed to the NO_3 reaction with HCs, attaining 17.0%. During daytime, from 08:00 to 17:00 BJT, the homogeneous pathway accounts for 89.9% of the HNO_3 production on average. The P_{HNO_3} increases with enhancement of solar radiation in the morning and peaks around noontime. The heterogeneous pathway plays an appreciable

role in the daytime HNO_3 production, with a contribution of 10.1%. The P_{HNO_3} of the heterogeneous pathway increases rapidly after sunset, peaks at approximately 20:00 BJT, and then drops slowly, which is caused mainly by decrease of O_3 due to continuous NO_x emissions during nighttime.

4 Conclusion

In the study, a source-oriented WRF-Chem model is developed and used to simulate a heavy haze episode from 16 to 31 December 2016 in the NCP, to verify contributions of the homogeneous and heterogeneous pathways to nitrate aerosols. The nitrate homogeneous pathway includes reactions of OH with NO_2 and NO_3 with HCs, and the heterogeneous pathway is referred to as the N_2O_5 hydrolysis uptake on surfaces of deliquescence aerosols. The model generally performs well in simulating meteorological parameters, air pollutants and inorganic aerosols against observations in the NCP.

On average, during the episode in the NCP, the homogeneous and heterogeneous pathways contribute 48.4% and 51.6% of the near-surface nitrate mass, respectively. During nighttime, the N_2O_5 hydrolysis dominates the HNO_3 formation in the PBL, with a contribution of 83.6%, while the homogeneous pathway accounts for 89.9% of daytime HNO_3 formation. The homogeneous and heterogeneous pathways play almost same role in the HNO_3 formation in the PBL. It is worth noting that the N_2O_5 hydrolysis also plays an appreciable role in the daytime HNO_3 formation, with an average contribution of 10.1%, particularly under conditions with weak sunlight. Our research highlights the significant importance of the heterogeneous pathway to nitrate formation.

Acknowledgments. The observations of meteorological parameters are obtained from the

website <http://www.meteomanz.com>. The hourly observations of PM_{2.5}, O₃, SO₂, NO₂, and CO concentrations are released by Ministry of Ecology and Environment of China and can be downloaded from the website <http://106.37.208.233:20035>. This work is financially supported by the National Key R&D Plan (Quantitative Relationship and Regulation Principle between Regional Oxidation Capacity of Atmospheric and Air Quality (2017YFC0210000)) and National Research Program for Key Issues in Air Pollution Control (DQGG0105). The authors would like to acknowledge helpful discussions with Professor Jianlin Hu.

249 References

- 250 An, Z. S., Huang, R. J., Zhang, R. Y., Tie, X. X., Li, G. H., Cao, J. J., et al. (2019). Severe haze in northern
251 China: A synergy of anthropogenic emissions and atmospheric processes. *Proceedings of the National*
252 *Academy of Sciences of the United States of America*, 116, 8657-8666.
253 <https://doi.org/10.1073/pnas.1900125116>.
- 254 Bei, N., Wu, J., Elser, M., Feng, T., Cao, J., El-Haddad, I., et al. (2017). Impacts of meteorological
255 uncertainties on the haze formation in Beijing–Tianjin–Hebei (BTH) during wintertime: a case study.
256 *Atmospheric Chemistry and Physics*, 17, 14579–14591. <https://doi.org/10.5194/acp-17-14579-2017>.
- 257 Bertram, T. H. & Thornton, J. A. (2009). Toward a general parameterization of N₂O₅ reactivity on aqueous
258 particles: the competing effects of particle liquid water, nitrate and chloride. *Atmospheric Chemistry*
259 *and Physics*, 9, 8351–8363. <https://doi.org/10.5194/acp-9-8351-2009>.
- 260 Brown, S. S., Dubé, W. P., Tham, Y. J., Zha, Q., Xue, L., Poon, S., et al. (2016). Nighttime chemistry at a
261 high altitude site above Hong Kong. *Journal of Geophysical Research–Atmospheres*, 121, 2457–2475.
262 <https://doi.org/10.1002/2015JD024566>.
- 263 Chang, W. L., Bhawe, P. V., Brown, S. S., Riemer, N., Stutz, J., & Dabdub, D. (2011). Heterogeneous
264 Atmospheric Chemistry, Ambient Measurements, and Model Calculations of N₂O₅: A Review.
265 *Aerosol Science and Technology*, 45, 665–695. <https://doi.org/10.1080/02786826.2010.551672>.
- 266 Chang, W. L., Brown, S. S., Stutz, J., Middlebrook, A. M., Bahreini, R., Wagner, N. L., et al. (2016).
267 Evaluating N₂O₅ heterogeneous hydrolysis parameterizations for CalNex 2010. *Journal of*
268 *Geophysical Research–Atmospheres*, 121, 5051–5070. <https://doi.org/10.1002/2015JD024737>.
- 269 Foley, K. M., Roselle, S. J., Appel, K. W., Bhawe, P. V., Pleim, J.E., Otte, T. L., et al. (2010). Incremental
270 testing of the Community Multiscale Air Quality(CMAQ) modeling system version 4.7. *Geoscientific*
271 *Model Development*, 3,205–226. <https://doi.org/10.5194/gmd-3-205-2010>.
- 272 Grell, G. A., Peckham, S. E., Schmitz, R., McKeen, S. A., Frost, G., Skamarock, W. C., et al. (2005). Fully
273 coupled “online” chemistry within the WRF model. *Atmospheric Environment*, 39, 6957–6975.
274 <https://doi.org/10.1016/j.atmosenv.2005.04.027>.
- 275 Guo, S., Hu, M., Zamora, M. L., Peng, J., Shang, D., Zheng, J., et al. (2014). Elucidating severe urban haze
276 formation in China. *Proceedings of the National Academy of Sciences of the United States of America*,
277 111, 17373–17378. <https://doi.org/10.1073/pnas.1419604111>.
- 278 Hu, J., Howard, C. J., Mitloehner, F., Green, P. G., & Kleeman, M. J. (2012). Mobile source and livestock
279 feed contributions to regional ozone formation in Central California. *Environmental Science*
280 *& Technology*, 46, 2781–2789. <https://doi.org/10.1021/es203369p>.
- 281 Hu, J., Wang, P., Ying, Q., Zhang, H., Chen, J., Ge, X., et al. (2017). Modeling biogenic and anthropogenic
282 secondary organic aerosol in China. *Atmospheric Chemistry and Physics*, 17, 77–92.
283 <https://doi.org/10.5194/acp-17-77-2017>.
- 284 Hu, J., Wu, L., Zheng, B., Zhang, Q., He, K., Chang, Q., et al. (2015). Source contributions and regional
285 transport of primary particulate matter in China. *Environmental Pollution*, 207, 31–42.
286 <https://doi.org/10.1016/j.envpol.2015.08.037>.
- 287 IPCC (Intergovernmental Panel on Climate Change). (2013). Climate Change 2013: The Physical Science
288 Basis. Contribution of Working Group I to the Fifth Assessment Report of the Intergovernmental
289 Panel on Climate Change. Cambridge University Press, New York, 571-657.
- 290 Kim, Y. J., Spak, S. N., Carmichael, G. R., Riemer, N., & Stanier, C. O. (2014). Modeled aerosol nitrate
291 formation pathways during wintertime in the Great Lakes region of North America. *Journal of*
292 *Geophysical Research–Atmospheres*, 119, 12420–12445. <https://doi.org/10.1002/2014JD022320>.
- 293 Lelieveld, J., Evans, J. S., Fnais, M., Giannadaki, D., & Pozzer, A. (2015). The contribution of outdoor air
294 pollution sources to premature mortality on a global scale. *Nature*, 525, 367-371.
295 <https://doi.org/10.1038/nature15371>.

296 Li, G., Bei, N., Tie, X., & Molina, L. T. (2011a). Aerosol effects on the photochemistry in Mexico City
 297 during MCMA-2006/MILAGRO campaign. *Atmospheric Chemistry and Physics*, 11, 5169–5182.
 298 <https://doi.org/10.5194/acp-11-5169-2011>.

299 Li, G., Lei, W., Bei, N., & Molina, L. T. et al. (2012). Contribution of garbage burning to chloride and
 300 PM_{2.5} in Mexico City. *Atmospheric Chemistry and Physics*, 12, 8751–8761.
 301 <https://doi.org/10.5194/acp-12-8751-2012>.

302 Li, G., Lei, W., Zavala, M., Volkamer, R., Dusanter, S., Stevens, P., et al. (2010). Impacts of HONO
 303 sources on the photochemistry in Mexico City during the MCMA-2006/MILAGO Campaign.
 304 *Atmospheric Chemistry and Physics*, 10, 6551–6567. <https://doi.org/10.5194/acp-10-6551-2010>.

305 Li, G., Zavala, M., Lei, W., Tsimpidi, A. P., Karydis, V. A., Pandis, S. N., et al. (2011b). Simulations of
 306 organic aerosol concentrations in Mexico City using the WRF-Chem model during the
 307 MCMA-2006/MILAGRO campaign. *Atmospheric Chemistry and Physics*, 11, 3789–3809.
 308 <https://doi.org/10.5194/acp-11-3789-2011>.

309 Liu, L., Wu, J., Liu, S., Li, X., Zhou, J., Feng, T., et al. (2019). Effects of organic coating on the nitrate
 310 formation by suppressing the N₂O₅ heterogeneous hydrolysis: a case study during wintertime in
 311 Beijing–Tianjin–Hebei (BTH). *Atmospheric Chemistry and Physics*, 19, 8189–8207.
 312 <https://doi.org/10.5194/acp-19-8189-2019>.

313 Lowe, D., Archer-Nicholls, S., Morgan, W., Allan, J., Utembe, S., Ouyang, B., et al. (2015). WRF-Chem
 314 model predictions of the regional impacts of N₂O₅ heterogeneous processes on night-time chemistry
 315 over north-western Europe. *Atmospheric Chemistry and Physics*, 15, 1385–1409.
 316 <https://doi.org/10.5194/acp-15-1385-2015>.

317 Nenes, A., Pandis, S. N., & Pilinis, C. (1998). ISORROPIA: A new thermodynamic equilibrium model for
 318 multiphase multicomponent inorganic aerosols. *Aquat Geochem*, 4, 123–152.
 319 <https://doi.org/10.1023/a:1009604003981>.

320 Qiao, X., Ying, Q., Li, X., Zhang, H., Hu, J., Tang, Y., et al. (2018). Source apportionment of PM_{2.5} for 25
 321 Chinese provincial capitals and municipalities using a source-oriented Community Multiscale Air
 322 Quality model. *Science of the Total Environment*, 612, 462–471.
 323 <http://dx.doi.org/10.1016/j.scitotenv.2017.08.272>.

324 Riemer, N., Vogel, H., Vogel, B., Schell, B., Ackermann, I., Kessler, C., et al. (2003). Impact of the
 325 heterogeneous hydrolysis of N₂O₅ on chemistry and nitrate aerosol formation in the lower troposphere
 326 under photochemical conditions. *Journal of Geophysical Research–Atmospheres*, D4, 4144.
 327 <https://doi.org/10.1029/2002JD002436>.

328 Riemer, N., Vogel, H., Vogel, B., Anttila, T., Kiendler-Scharr, A., & Mentel, T. F. (2009). Relative
 329 importance of organic coatings for the heterogeneous hydrolysis of N₂O₅ during summer in Europe.
 330 *Journal of Geophysical Research–Atmospheres*, D17307. <https://doi.org/10.1029/2008JD011369>.

331 Sun, Y. L., Wang, Z. F., Du, W., Zhang, Q., Wang, Q. Q., Fu, P. Q., et al. (2015). Long-term real-time
 332 measurements of aerosol particle composition in Beijing, China: seasonal variations, meteorological
 333 effects, and source analysis. *Atmospheric Chemistry and Physics*, 15, 10149–10165.
 334 <https://doi.org/10.5194/acp-15-10149-2015>.

335 Tao, J., Zhang, L., Cao, J., & Zhang, R. (2017). A review of current knowledge concerning PM_{2.5} chemical
 336 composition, aerosol optical properties and their relationships across China, *Atmospheric Chemistry
 337 and Physics*, 17, 9485–9518. <https://doi.org/10.5194/acp-17-9485-2017>.

338 Wang, H., Lu, K., Chen, X., Zhu, Q., Chen, Q., Guo, S., et al. (2017). High N₂O₅ concentrations observed
 339 in urban Beijing: Implications of a large nitrate formation pathway. *Environmental Science
 340 & Technology Letters*, 4, 416–420. <https://doi.org/10.1021/acs.estlett.7b00341>.

341 Wang, P., Ying, Q., Zhang, H., Hu, J., Lin, Y., & Mao, H. (2018). Source apportionment of secondary
 342 organic aerosol in China using a regional source-oriented chemical transport model and two emission
 343 inventories. *Environmental Pollution*, 237, 756–766. <https://doi.org/10.1016/j.envpol.2017.10.122>

- Wang, Y. L., Song, W., Yang, W., Sun, X. C., Tong, Y. D., Wang, X. M., et al. (2019). Influences of atmospheric pollution on the contributions of major oxidation pathways to PM_{2.5} nitrate formation in Beijing. *Journal of Geophysical Research–Atmospheres*, 124, 4174–4185. <https://doi.org/10.1029/2019JD030284>.
- Xue, J., Yuan, Z., Lau, A. K. H., & Yu, J. Z. (2014). Insights into factors affecting nitrate in PM_{2.5} in a polluted high NO_x environment through hourly observations and size distribution measurements. *Journal of Geophysical Research–Atmospheres*, 119, 4888–4902. <https://doi.org/10.1002/2013JD021108>.
- Ying, Q., Feng, M., Song, D., Wu, L., Hu, J., Zhang, H., et al. (2018). Improve regional distribution and source apportionment of PM_{2.5} trace elements in China using inventory-observation constrained emission factors. *Science of the Total Environment*, 624, 355–365. <https://doi.org/10.1016/j.scitotenv.2017.12.138>.
- Ying, Q., & Kleeman, M. J. (2006). Source contributions to the regional distribution of secondary particulate matter in California. *Atmospheric Environment*, 40, 736–752. <https://doi.org/10.1016/j.atmosenv.2005.10.007>.
- Ying, Q., & Krishnan, A. (2010). Source contributions of volatile organic compounds to ozone formation in southeast Texas. *Journal of Geophysical Research–Atmospheres*, 115, D17306. <https://doi.org/10.1029/2010JD013931>.
- Zhang, H., & Ying, Q. (2011). Contributions of local and regional sources of NO_x to ozone concentrations in Southeast Texas. *Atmospheric Environment*, 45, 2877–2887. <https://doi.org/10.1016/j.atmosenv.2011.02.047>.
- Zhang Q., Zheng Y., Tong, D., Shao, M., Wang, S., Zhang, Y., et al. (2019). Drivers of improved PM_{2.5} air quality in China from 2013 to 2017. *Proceedings of the National Academy of Sciences of the United States of America*, 116(49), 24463–24469. <https://doi.org/10.1073/pnas.1907956116>.
- Zhang, R., Jing, J., Tao, J., Hsu, S., Wang, G., Cao, J., et al. (2013). Chemical characterization and source apportionment of PM_{2.5} in Beijing: seasonal perspective. *Atmospheric Chemistry and Physics*, 13, 7053–7074. <https://doi.org/10.5194/acp-13-7053-2013>.
- Zheng, B., Tong, D., Li, M., Liu, F., Hong, C., Geng, G., et al. (2018). Trends in China's anthropogenic emissions since 2010 as the consequence of clean air actions. *Atmospheric Chemistry and Physics*, 14095–14111. <https://doi.org/10.5194/acp-18-14095-2018>.

Figure Captions

- Figure 1 Conceptual scheme of source apportionment for the nitrate formation pathway. A: homogenous pathway; B: heterogeneous pathway; Subscript g : gas phase; Subscript a : aerosol phase; Superscript T : total; $S(+VI)_a$: sulfate; $N(+V)_a$: nitrate aerosol; $N(+V)_g$: nitric acid; $N(-III)_a$: ammonium aerosol; $N(-III)_g$: ammonia; t : current time; δt : integration time step.
- Figure 2 Simulated diurnal profiles of the average near-surface nitrate concentration from the homogeneous and heterogeneous pathways in the NCP from 16 to 31 December 2016.
- Figure 3 Spatial distributions of average near-surface nitrate concentrations from the (a) homogeneous and (b) heterogeneous pathway in the NCP from 16 to 31 December 2016.
- Figure 4 Simulated temporal variations of the average *in-situ* HNO_3 production rate of the homogeneous and heterogeneous pathways in the PBL over the NCP from 16 to 31 December 2016.
- Figure 5 Diurnal cycle of the average *in-situ* HNO_3 production rate of the (a) homogeneous and (b) heterogeneous pathway in the PBL over NCP from 16 to 31 December 2016.

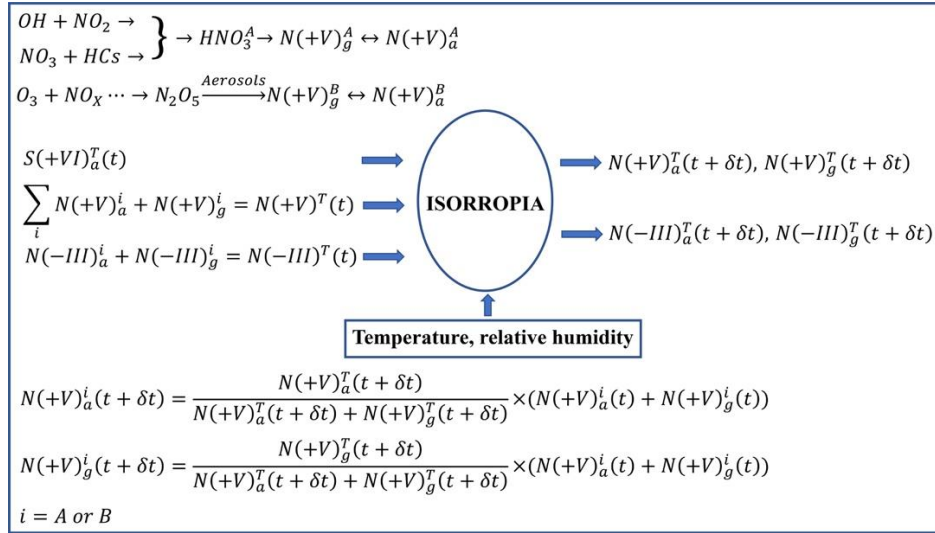


Figure 1 Conceptual scheme of source apportionment for the nitrate formation pathway. A: homogenous pathway; B: heterogeneous pathway; Subscript *g*: gas phase; Subscript *a*: aerosol phase; Superscript *T*: total; $S(+VI)_a$: sulfate aerosol; $N(+V)_a$: nitrate aerosol; $N(+V)_g$: nitric acid; $N(-III)_a$: ammonium aerosol; $N(-III)_g$: ammonia; *t*: current time; δt : integration time step.

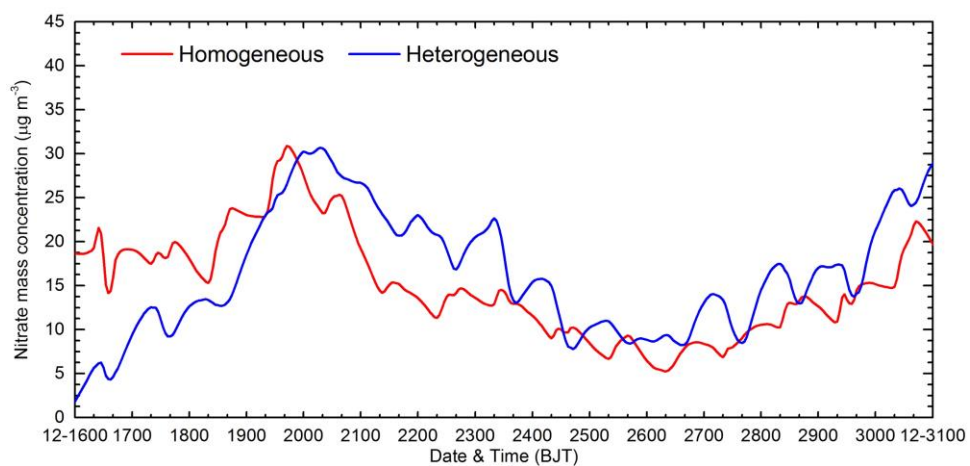


Figure 2 Simulated diurnal profiles of the average near-surface nitrate concentration from the homogeneous and heterogeneous pathways in the NCP from 16 to 31 December 2016.

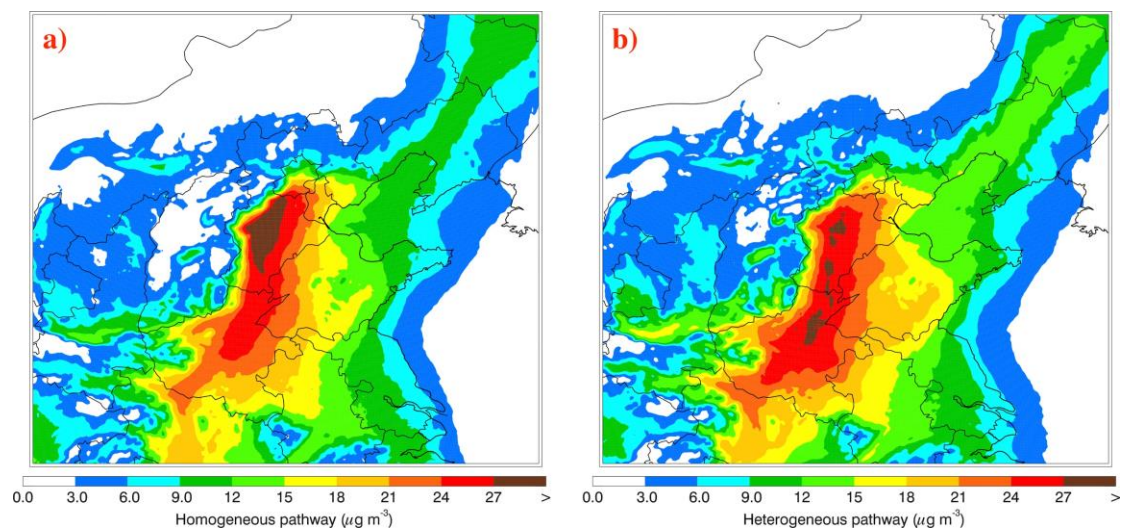


Figure 3 Spatial distributions of average near-surface nitrate concentrations from the (a) homogeneous and (b) heterogeneous pathway in the NCP from 16 to 31 December 2016.

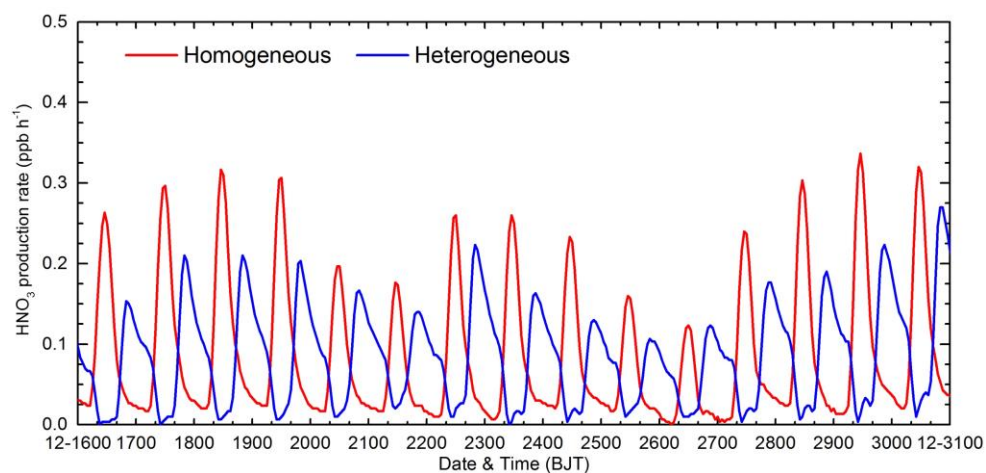


Figure 4 Simulated temporal variations of the average *in-situ* HNO₃ production rate of the homogeneous and heterogeneous pathways in the PBL over the NCP from 16 to 31 December 2016.

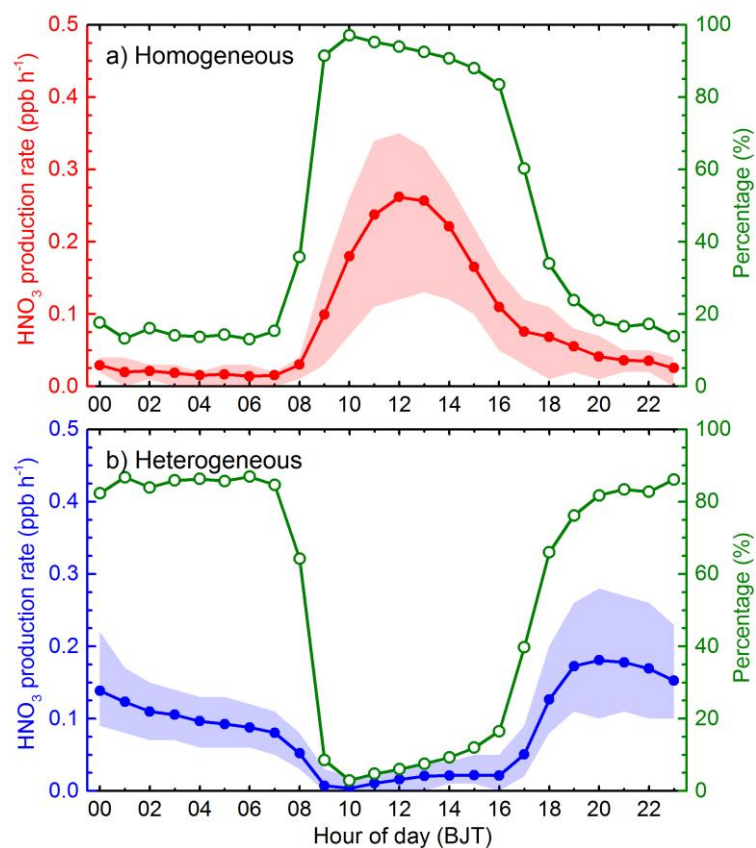


Figure 5 Diurnal cycle of the average *in-situ* HNO₃ production rate of the (a) homogeneous and (b) heterogeneous pathway in the PBL over NCP from 16 to 31 December 2016.